iScience

CellPress
OPEN ACCESS

Article

The *Drosophila* microRNA bantam regulates excitability in adult mushroom body output neurons to promote early night sleep

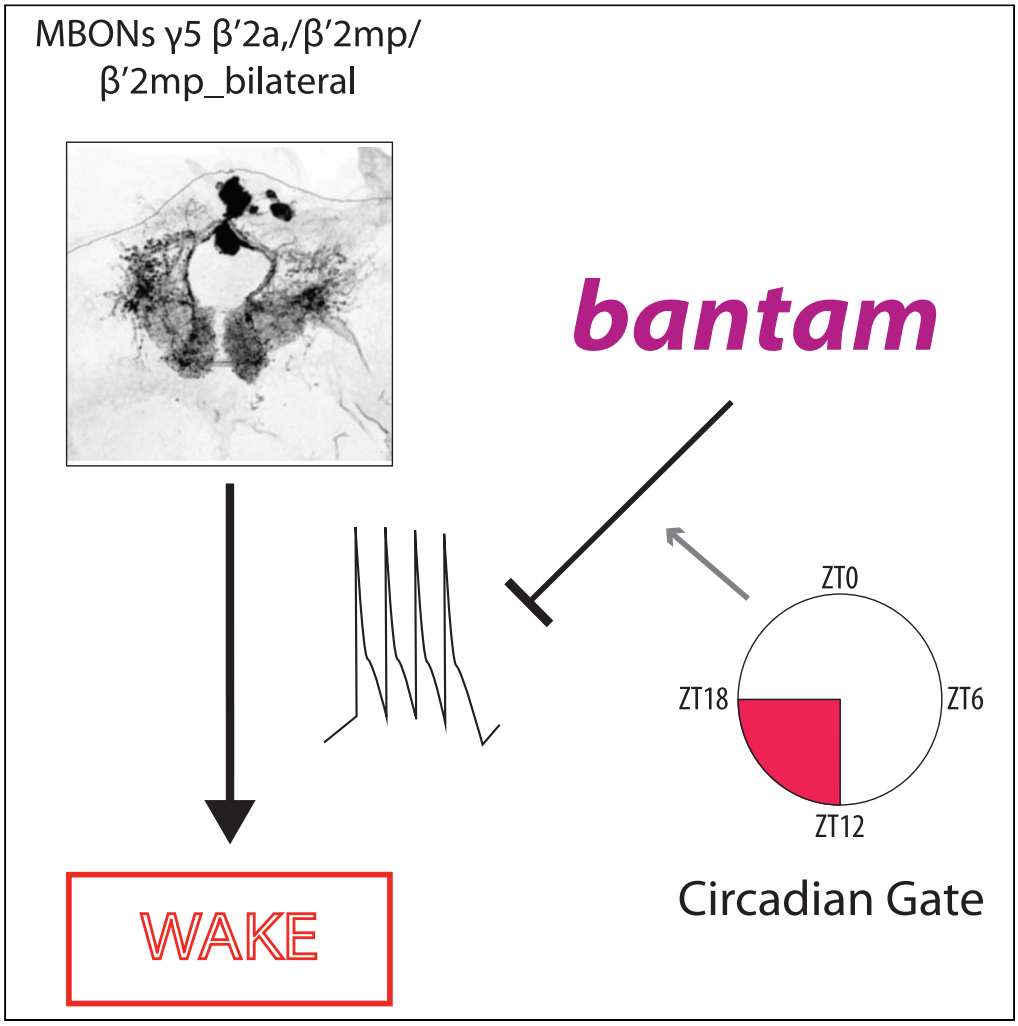

Michael Hobin, Katherine Dorfman, Mohamed Adel, Emmanuel J. Rivera-Rodriguez, Elena A. Kuklin, Dingbang Ma, Leslie C. Griffith

griffith@brandeis.edu

Highlights

The *bantam* microRNA has both developmental and adult roles in the regulation of sleep

Bantam promotes early nighttime sleep in adult 5β′2a/β′2mp/β′2mp_bilateral MBONs

Bantam suppresses MBON neuronal activity specifically in the early nighttime

Suppressing activity of 5β′2a/β′2mp/β′2mp_bilateral MBONs rescues *ban* knockdown

Hobin et al., iScience *25*, 104874
September 16, 2022
https://doi.org/10.1016/j.isci.2022.104874

iScience

CellPress
OPEN ACCESS

Article

The *Drosophila* microRNA bantam regulates excitability in adult mushroom body output neurons to promote early night sleep

Michael Hobin,[1] Katherine Dorfman,[1,3] Mohamed Adel,[1] Emmanuel J. Rivera-Rodriguez,[1] Elena A. Kuklin,[1] Dingbang Ma,[1,2] and Leslie C. Griffith[1,4,*]

SUMMARY

Sleep circuitry evolved to have both dedicated and context-dependent modulatory elements. Identifying modulatory subcircuits and understanding their molecular machinery is a major challenge for the sleep field. Previously, we identified 25 sleep-regulating microRNAs in *Drosophila melanogaster*, including the developmentally important microRNA *bantam*. Here we show that *bantam* acts in the adult to promote early nighttime sleep through a population of glutamatergic neurons that is intimately involved in applying contextual information to behaviors, the γ5β′2a/β′2mp/β′2mp_bilateral Mushroom Body Output Neurons (MBONs). Calcium imaging revealed that bantam inhibits the activity of these cells during the early night, but not the day. Blocking synaptic transmission in these MBONs rescued the effect of *bantam* knockdown. This suggests *bantam* promotes early night sleep via inhibition of the γ5β′2a/β′2mp/β′2mp_bilateral MBONs. RNAseq identifies *Kelch* and *CCHamide-2 receptor* as possible mediators, establishing a new role for *bantam* as an active regulator of sleep and neural activity in the adult fly.

RESULTS

Bantam promotes nighttime sleep via the γ5β′2a/β′2mp/β′2mp_bilateral MBONs

To investigate the roles of *bantam (ban)* in sleep, we utilized a previously validated (Becam et al., 2011) microRNA sponge transgene to reduce its levels. The technique allows spatially- and temporally-specific interrogation of the roles of microRNAs (Fulga et al., 2015). We had previously shown that pan-neuronal (with *nSyb-GAL4*) expression of the *bantam* sponge *(ban-SP)* led to a reduction in sleep (Goodwin et al., 2018), indicating that *ban* acts in the nervous system to promote sleep. Because sleep-regulating genes can exert their effects at different stages throughout the lifespan of an animal, as developmental regulators contributing to the formation of sleep circuits (Chakravarti Dilley et al., 2020; Gong et al., 1998; Xie et al., 2019) or as active regulators of adult sleep (for review see Crocker and Sehgal, 2010), it was important to determine the temporal window of *ban* action. We made use of an inducible expression system to control sponge expression. *ban-SP* was placed under the control of the pan-neuronal driver *nSyb-GAL4* and a ubiquitously expressed temperature-sensitive inhibitor of GAL4 activity-*tubulin-GAL80^{ts}* (McGuire et al., 2003). In this genotype, *ban-SP* is expressed at 29°C, but not at 17–18°C. Female *nSyb>ban-SP, tubulin-GAL80^{ts}* flies were raised at 17°C and then shifted to 29°C after eclosion and for the duration of the sleep assay. Adult-specific pan-neuronal knockdown of *ban* led to a significant reduction in daytime and nighttime sleep compared to control animals expressing a scrambled sponge transgene (*UAS-scr-SP*) (Figure 1A). This reduction was most prominent in the early night, ZT12-18 (Figure 1A). In contrast, developmental knockdown of *ban* led to a significant reduction in daytime, but not nighttime, sleep (Figure S1A). These results indicate that in the adult brain, *ban* acts acutely to promote early night sleep. Consistent with this, pan-neuronal overexpression of *ban* increased sleep (Figure S1B).

We next sought to localize the effect of *ban* on sleep to a specific population of neurons. We expressed *CD8::GFP* under the control of the *ban-GAL4* driver to examine the expression pattern of *ban* in the adult brain (Figure 1B). Immunohistochemistry of *ban>CD8::GFP* brains revealed high GFP staining in both

[1]Department of Biology, Volen National Center for Complex Systems, Brandeis University, Waltham, MA 02454-9110, USA

[2]Howard Hughes Medical Institute, Brandeis University, Waltham, MA 02454-9110, USA

[3]Present address: Perelman School of Medicine at the University of Pennsylvania, Philadelphia, PA 19104, USA

[4]Lead contact

*Correspondence: griffith@brandeis.edu

https://doi.org/10.1016/j.isci.2022.104874

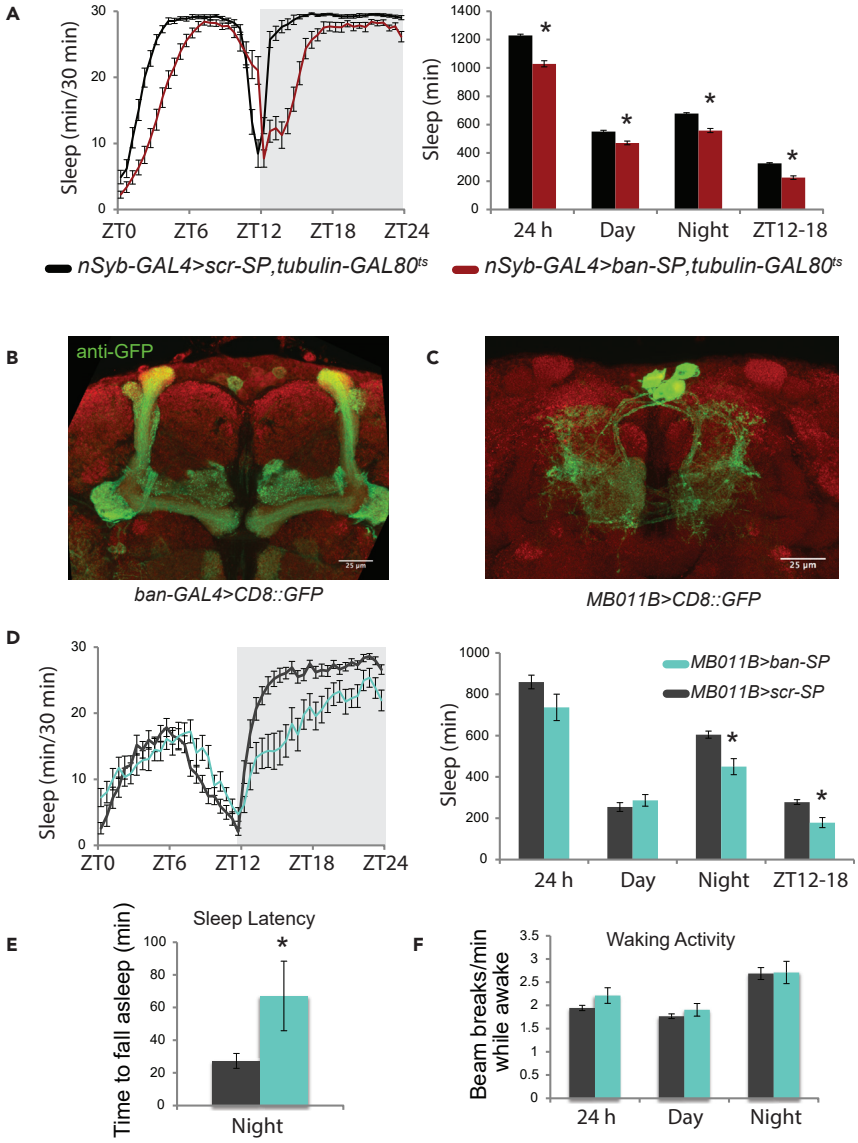

Figure 1. Bantam promotes nighttime sleep via the γ5β′2a/β′2mp/β′2mp_bilateral MBONs

(A) Adult-specific knockdown of ban. Sleep data for *nSyb>ban-SP, tubulin-GAL80^{ts}* (N = 27) and scramble controls (N = 31) raised at 17°C and tested at 29°C (mean ± SEM). * represents p ≤ 0.0001, Mann-Whitney-Wilcoxon test or unpaired t-test.

(B) Anti-GFP staining (green) for the central brain of a representative *ban>CD8::GFP* fly (63X). Anti-BRP (nc82) was used to stain neuropil (red). Scale bar measures 25μm.

(C) Anti-GFP (green) and anti-BRP (red) staining for the brain of a representative *MB011B>UAS-CD8::GFP* fly (63X). Scale bar measures 25μm.

(D) Sleep data for *MB011B>ban-SP* (N = 17) and scramble controls (N = 24) shown as mean ± SEM * represents p ≤ 0.0005, unpaired t-test.

(E) Sleep latency for same animals (minutes to fall asleep after lights out) shown as mean ± SEM * represents p ≤ 0.05, unpaired t-test.

(F) Beam breaks per active minute (general locomotor activity) for same animals (mean ± SEM).

the intrinsic and extrinsic cells of the mushroom body (MB; Figure 1B), a centrally located neuropil with a well-characterized role in *Drosophila* sleep (Joiner et al., 2006; Pitman et al., 2006). The mushroom body scaffold is composed of the axonal projections of Kenyon cells (intrinsic cells), which communicate with several populations of extrinsic cells. The primarily input cell type is dopaminergic (Mao and Davis, 2009) whereas the primary output of Kenyon cells is via synapses onto the dendrites of Mushroom Body Output

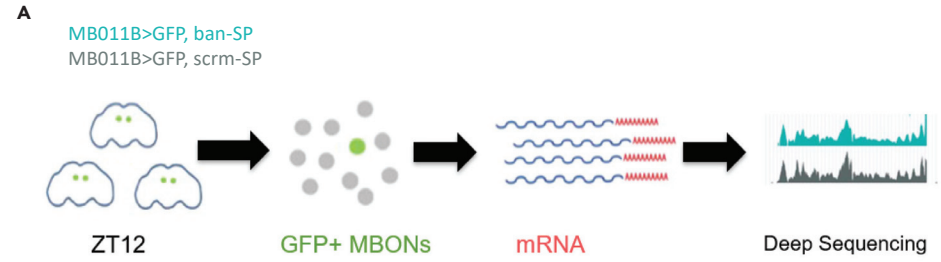

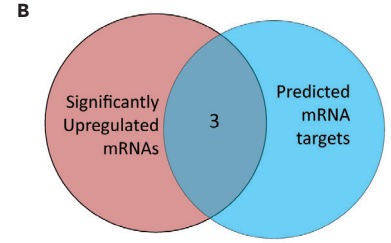

Upregulated Predicted target mRNA	Gene Summary	edgeR DGE p-value
Ugt36D1	glycosyltransferase	0.018628168
Kelch	ubiquitin ligase adaptor	0.042747249
CCHa2R	GPCR neuropeptide receptor	0.00156062

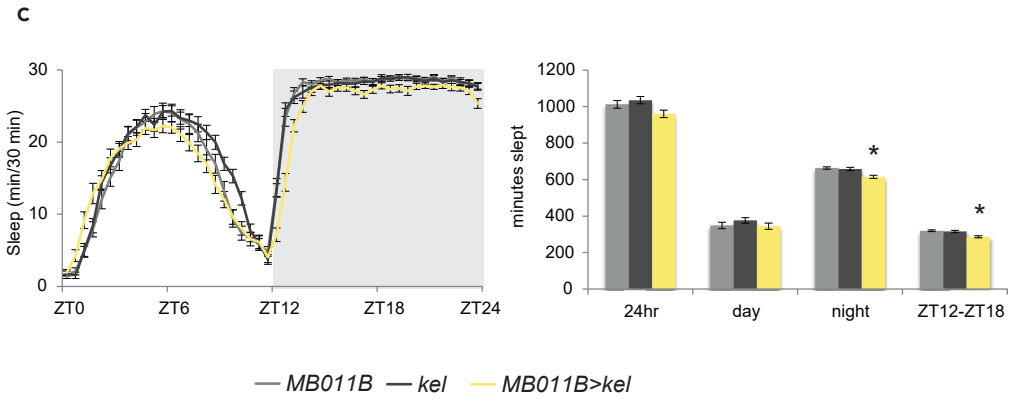

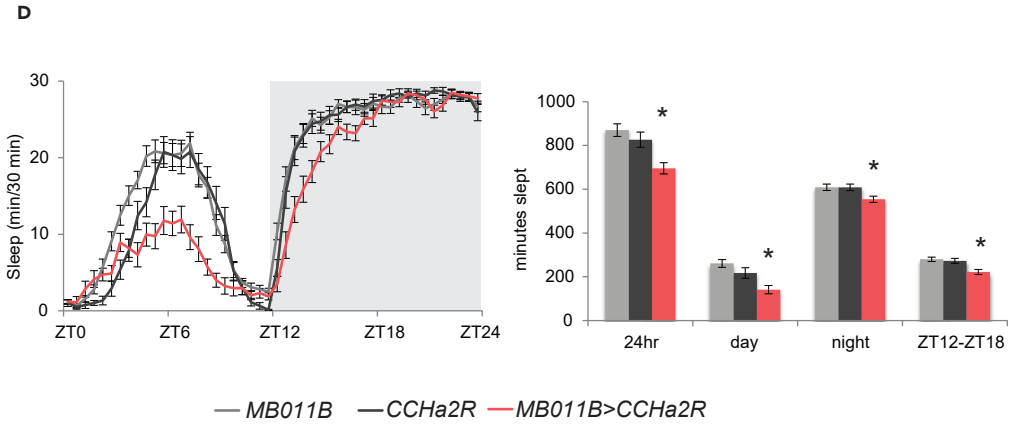

Figure 2. Bantam negatively regulates wake-promoting genes in the γ5β′2a/β′2mp/β′2mp_bilateral MBONs

(A) Schematic diagram of the MBON purification and sequencing paradigm.

(B) Venn diagram representing selection criteria for putative *ban* microRNA targets in the γ5β′2a/β′2mp/β′2mp_bilateral MBONs. Table representing the three "hits", their gene summarizations and their p-value significance for edgeR differential gene expression analysis.

(C) Sleep data for *MB011B>kel* (n = 31), *MB011B* control (n = 32) and *UAS-kel* control (n = 28) (mean ± SEM). * represents $p \leq 0.001$, Kruskal-Wallis test with Dunn's multiple comparison test.

Figure 2. *Continued*
(D) Sleep data for *MB011B>CCHa2-R* (n = 23), *MB011B* control (n = 27) and *UAS-CCHa2-R* control (n = 22) (mean ± SEM). * represents $p \leq 0.05$, Kruskal-Wallis test with Dunn's multiple comparison test or one-way ANOVA with Tukey's multiple comparisons test.

Neurons (MBONs) (Aso et al., 2014a). Given the high expression level of *ban-GAL4* in the MB, we first examined whether *ban* expression in Kenyon cells was necessary for normal sleep. Expression of *ban-SP* under the powerful Kenyon cell driver *OK107-GAL4* had no effect on sleep (Figure S1C), indicating that *ban* does not regulate sleep through MB intrinsic cells. We next tested the effect of *ban* knockdown on dopaminergic neurons. Expression of *ban-SP* under the dopaminergic driver *TH-GAL4* also had no effect on nighttime sleep, although it did lead to a small increase in daytime sleep (Figure S1D). These negative results directed our attention to the third major component of the mushroom body circuit-the MBONs.

The MBONs consist of 21 subtypes divided into three classes determined by neurotransmitter identity (GABA, acetylcholine and glutamate) with each MBON named on the basis of the MB lobe section(s) which it innervates (Aso et al., 2014a). Several MBON subtypes have been implicated in sleep regulation, including the glutamatergic γ5β′2a/β′2mp/β′2mp_bilateral MBONs (Figure 1B) which have been previously shown to inhibit sleep when activated (Aso et al., 2014a; Sitaraman et al., 2015). To test if *ban* regulates sleep via this cell type, we drove *ban-SP* with the *MB011B* split-GAL4. *MB011B>ban-SP* flies exhibited a significant reduction in nighttime sleep (Figures 1D and S1E), in addition to increased sleep latency (Figure 1E) compared to animals expressing a control scrambled sponge (*scr-SP*). Nighttime sleep loss was most severe in the early night ZT12-18 period (Figure 1D). Driving *ban-SP* with an independent GAL4 line, GMR14C08, which has expression in this same subset of MBONs, also caused early night sleep loss (see Figure 3F, top panel). Interestingly, in contrast to the pan-neuronal adult knockdown results, *ban* knockdown in these MBONs had no effect on daytime sleep, indicating that the daytime sleep regulatory role of *ban* is likely mediated by different neurons. Importantly, knockdown of *ban* in the γ5β′2a/β′2mp/β′2mp_bilateral MBONs had no effect on waking motor activity (Figure 1F), demonstrating that the effect of this microRNA was specific to sleep rather than affecting general motor behavior.

Bantam negatively regulates wake-promoting genes in the γ5β′2a/β′2mp/β′2mp_bilateral MBONs

MicroRNAs exert their effects on cellular functions via inhibition of target mRNAs either through transcript degradation or translational silencing (Jonas and Izaurralde, 2015). MicroRNA knockdown leads to increased expression of its target mRNAs, either through increased RNA stability, translation or both. Knockdown of *ban* in the γ5β′2a/β′2mp/β′2mp_bilateral MBONs should therefore lead to upregulation of *ban* target mRNAs. To identify candidate targets of *ban*, we performed fluorescence-activated cell sorting (FACS) and deep sequencing on γ5β′2a/β′2mp/β′2mp_bilateral MBONs expressing GFP and *ban-SP* or *scr-SP*. Adult brains were dissected in the ZT12-13:30 time window (the time of maximum sleep-loss- Figure 1D). GFP+ MBONs were isolated by FACS and total mRNA was sequenced using a modified SMART-seq2 protocol (Liu et al., 2017; Picelli et al., 2014). RNA sequencing and Differential Gene Expression edgeR analysis (Robinson et al., 2010) for three biological replications was then performed to identify mRNAs that were significantly upregulated in the *ban* knockdown condition (Figure 2A). The list of statistically significant upregulated genes was compared to lists of putative target mRNAs generated by two microRNA-mRNA target prediction algorithms, TargetscanFly7.2 (Agarwal et al., 2018; Ruby et al., 2007) and DIANA-microT (Paraskevopoulou et al., 2013; Reczko et al., 2012). This pipeline produced 3 candidate mRNAs that were both significantly upregulated in the *ban* knockdown condition and were predicted direct targets- *UDP-glycosyltransferase family 36 member D1 (Ugt36D1)*, *Kelch (kel)* and *CCHamide-2 receptor (CCHa2-R)* (Figure 2B).

To determine if upregulation of these mRNAs contributes to the *ban* sleep loss phenotype, we overexpressed these genes within the γ5β′2a/β′2mp/β′2mp_bilateral MBONs and measured their effect on sleep. *MB011B>Ugt36D1* flies exhibited normal sleep (Figure S2A), but both *MB011B>kel* and *MB011B>CCHa2-R* flies exhibited small but statistically significant reductions in early nighttime sleep (Figures 2C and 2D). qPCR on *nsyb-GAL4>CCHa2-R* fly heads and parental line controls was used to verify the efficacy of the *UAS-CCHa2-R* transgene in driving GAL-4 dependent overexpression (Figure S2B); the *UAS-kelch* overexpression transgene was previously validated (Hudson et al., 2015). These results suggest that the negative

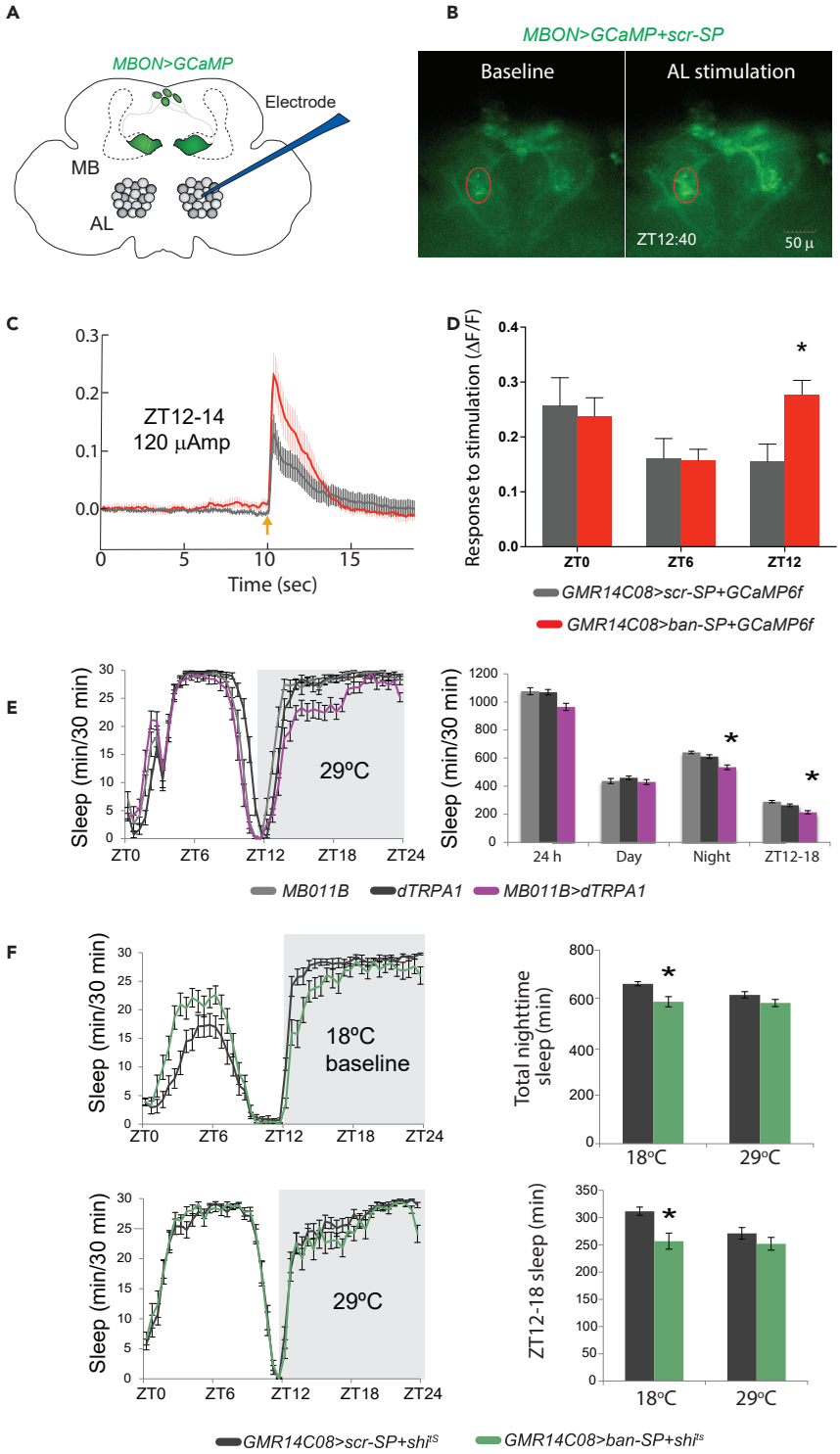

Figure 3. Bantam inhibits neural activity in the wake-promoting γ5β′2a/β′2mp/β′2mp_bilateral MBONs

(A) Schematic diagram of paradigm for antennal lobe (AL) microelectrode stimulation and γ5β′2a/β′2mp/β′2mp_bilateral MBON GCaMP6f recording. Dashed line represents mushroom body.

(B) GCaMP6f images showing representative dendritic Ca^{2+} responses of *GMR14C08>scr-SP+GCaMP6f* during baseline and after antennal lobe stimulation. Experiment was carried out at ZT12:40. 0.12mA stimulation was delivered. Scale bar measures 50µm.

Figure 3. *Continued*

(C) Average ΔF/F time course for Ca^{2+} responses of *GMR14C08>scr-SP+GCaMP6f* (gray) and *GMR14C08>ban-SP+-GCaMP6f* (red) dendrites to antennal lobe stimulation (orange arrow) in the ZT12-14 time window (mean ± SEM).

(D) ΔF/F for Ca^{2+} responses of *GMR14C08>scr-SP+GCaMP6f* (gray) and *GMR14C08>ban-SP+GCaMP6f* (red) dendrites to antennal lobe stimulation (0.12mA) in the ZT0-2, ZT6-8 and ZT12-14 time windows (mean ± SEM). * represents $p \leq 0.05$, two-way ANOVA and Sidak post hoc comparison. n = 8 for all groups.

(E) Sleep data for *MB011B>dTrpA1* (n = 31), *MB011B* control (n = 27) and *UAS-dTrpA1* control (n = 30) tested for sleep behavior at 29°C (mean ± SEM). * represents $p \leq 0.01$, Kruskal-Wallis test with Dunn's multiple comparison test.

(F) Sleep data for *GMR14C08>ban-SP+shi^{ts}* (n = 30) and *GMR14C08>scr-SP+shi^{ts}* (n = 31) tested at 18°C and 29°C (mean ± SEM). * represents $p \leq 0.01$, Mann-Whitney-Wilcoxon test.

regulation of these target mRNAs may contribute to the nighttime sleep-promoting effect of ban in the γ5β′2a/β′2mp/β′2mp_bilateral MBONs.

Bantam inhibits neural activity in the wake-promoting γ5β′2a/β′2mp/β′2mp_bilateral MBONs

Our results suggest that *ban* expression in the γ5β′2a/β′2mp/β′2mp_bilateral MBONs is required for normal early nighttime sleep. However, the underlying physiological processes regulated by *ban* within these neurons were unknown. Given the previously characterized role of *ban* in the regulation of cellular proliferation and differentiation (Banerjee and Roy, 2017; Brennecke et al., 2003; Lerner et al., 2015; Weng and Cohen, 2015), we asked whether knockdown of *ban* in γ5β′2a/β′2mp/β′2mp_bilateral MBONs led to an alteration in cell number or structure. Comparison of *MB011B>CD8::GFP+ban-SP* to control *MB011B>CD8::GFP+scr-SP* brains revealed no differences in GFP-positive cell number nor gross morphology (Figures S3A and S3B). These results suggest an adult role for *ban* in the regulation of behavior and cellular processes in the γ5β′2a/β′2mp/β′2mp_bilateral MBONs.

Given the apparent normality of the structure of these MBONs, we hypothesized that *ban* had a role in regulation of their activity. It had been previously shown that *dTrpA1*-induced (Hamada et al., 2008) neural activation of the γ5β′2a/β′2mp/β′2mp_bilateral MBONs reduces sleep (Aso et al., 2014a; Sitaraman et al., 2015). In this same study, suppression of transmitter release using a temperature-sensitive dominant negative dynamin transgene (*shibire^{ts}*) (Kitamoto, 2001), did not affect sleep, suggesting a model in which MBONs modify baseline sleep levels only as a response to salient information presented to the MB. Given that neuronal activation of the γ5β′2a/β′2mp/β′2mp_bilateral MBONs phenocopied the effect of *ban* knockdown on sleep, this suggested that knockdown of *ban* may increase the ability of these neurons to respond to stimuli. Consistent with this, we noted an increase in arousal at night, as measured by P(wake) (Wiggin et al., 2020), in animals with reduced *ban* function in these MBONs (Figure S1F).

To test the idea that *ban* regulates neuronal activity, we drove *GCaMP6f*, a calcium sensor, with *GMR14C08-GAL4*, a stronger driver for γ5β′2a/β′2mp/β′2mp_bilateral MBONs. MBONs are downstream of an excitatory pathway that conveys olfactory information to the MB circuit; antennal lobe (AL) projection neurons send excitatory inputs to Kenyon cells which in turn make excitatory connections on MBONs (Aso et al., 2014a; Barnstedt et al., 2016; Ueno et al., 2013). This excitatory pathway was activated by a glass suction microelectrode placed on a subset of AL neurons while calcium dynamics in the dendrites of the ipsilateral group of γ5β′2a/β′2mp/β′2mp_bilateral MBONs were recorded (Figures 3A and 3B) (Ueno et al., 2013, 2017; Wang et al., 2008). Consistent with our hypothesis, *GMR14C08>ban-SP+GCaMP6f* MBONs exhibited a significantly higher mean dendritic ΔF/F calcium response than control *GMR14C08>scr+GCaMP6f* MBONs when the AL was stimulated in the ZT12-14 window, the time of maximal sleep loss (Figures 3C and 3D). Because *ban* knockdown reduces sleep in a time-of-day-dependent manner we asked whether the effect of *ban* knockdown on responsiveness exhibited a similar pattern. Mirroring our behavioral results, AL stimulation at ZT0 and ZT6 produced calcium responses which were statistically indistinguishable from *scr-SP* controls (Figure 3D). These results demonstrate that *ban* negatively regulates the activity of the γ5β′2a/β′2mp/β′2mp_bilateral MBONs during the early night, but not during the day, in line with its effects on sleep.

To ask if the increased neuronal activity associated with *ban* knockdown was causally related to the sleep loss phenotype we first confirmed that activation of the γ5β′2a/β′2mp/β′2mp_bilateral MBONs with the temperature-sensitive cation channel *dTrpA1* decreased nighttime sleep (Figure 3E) and that inhibition

of MBON synaptic release with *shibire*^{ts} had no effect on baseline sleep (Figure S3C). We then hypothesized that if the increased responsiveness associated with *ban* knockdown was causative for the sleep loss phenotype, inhibition of γ5β′2a/β′2mp/β′2mp_bilateral MBON activity in *ban-SP*-expressing flies should rescue early night sleep. To test this, we co-expressed *ban-SP* with *shi*^{ts}. *GMR14C08>ban-SP+shi*^{ts} flies exhibited decreased nighttime sleep when tested at the permissive temperature of 18°C (Figure 3F), consistent with loss of *ban* activity. However, when tested at the restrictive temperature of 29°C (which blocks MBON synaptic signaling), *GMR14C08-GAL4>ban-SP+shi*^{ts} flies exhibited sleep levels statistically indistinguishable from *scr-SP* controls (Figure 3F). The ability of *shi*^{ts} to rescue the sleep loss phenotype indicates that *ban* knockdown enhances neurotransmission by MBONs which in turn inhibits nighttime sleep. These results demonstrate that *ban*-mediated control of neuronal activity within the wake-promoting γ5β′2a/β′2mp/β′2mp_bilateral MBONs acts to promote early nighttime sleep. In addition, the fact that the alternative γ5β′2a/β′2mp/β′2mp_bilateral MBON driver, *GMR14C08-GAL4*, produced a sleep-loss phenotype when expressing the *ban-SP* at the permissive temperature (Figure 3F) supports the idea that *ban* acts in this neuronal sub-population to regulate sleep.

DISCUSSION

MicroRNAs have emerged as key regulators of sleep and wake, but the cellular and physiological mechanisms via which individual microRNAs influence sleep remain largely uncharacterized. Here we show a new role for the microRNA *bantam (ban)* in promoting early nighttime sleep by decreasing the responsiveness of the wake-promoting γ5β′2a, β′2mp, β′2mp_bilateral MBONs. *ban* is a widely-expressed microRNA with well-characterized developmental roles in the specification of neuron number and morphology (Parrish et al., 2009; Song et al., 2012; Weng and Cohen, 2015). Known adult roles for *ban* have been largely limited to regulation of stem cells or other proliferative populations (Huang et al., 2014; Shcherbata et al., 2007) making the adult-specific role of *ban* in regulation of neuronal excitability a previously unrecognized function for this microRNA. It is important to note, however, that this is likely not the only way in which *ban* can affect sleep-its developmental functions contribute to adult daytime sleep generation and it appears to have a wake-promoting effect in dopaminergic cells (Figure S1).

Down-regulation of *ban* in the adult γ5β′2a, β′2mp, β′2mp_bilateral MBONs produces a sleep loss phenotype largely restricted to the early night ZT12-18 period as well as an increase in sleep latency. A number of sleep-regulating genes exhibit patterns of sleep loss that are largely confined to the early night period (Cong et al., 2015) or have large effects on latency (Agosto et al., 2008). Conversely, other sleep-regulating genes primarily contribute to late night sleep (Gmeiner et al., 2013; Kunst et al., 2014). This may reflect the fact that early and late-night sleep represent physiologically distinct states under differential genetic and neuroanatomical regulation and which likely serve different functions. Mammalian sleep varies across the night with slow-wave non-REM sleep predominant during the early night and REM sleep more frequent during the late night. Early and late night sleep has also been shown to facilitate different aspects of sleep-dependent memory processing (Plihal and Born, 1997; Yordanova et al., 2008). Our data show that *bantam* is important in allowing the initiation of early night sleep by suppressing activation of the γ5β′2a/β′2mp/β′2mp_bilateral MBONs.

Similar to mammalian sleep, *Drosophila* sleep is regulated by a widely distributed neural network (Shafer and Keene, 2021). The role of the mushroom body in the sculpting of responses to external conditions makes this structure uniquely suited to providing context-specific regulation of sleep. Consistent with this, synaptic silencing of the γ5β′2a/β′2mp/β′2mp_bilateral MBONs with *shi*^{ts} (this study and Sitaraman et al., 2015), electrical silencing (with *UAS-kir2.1*) and induced apoptosis (with *UAS-hid*) of the γ5β′2a/β′2mp/β′2mp_bilateral MBONs (MH, data not shown) have no effect on basal sleep. A similar sleep regulation pattern was demonstrated for the wake-promoting *C01+A05* neurons: knockdown of the calcium sensor *Neurocalcin* in these cells led to reduced sleep and increased neural activity, whereas electrical silencing of the cells had no effect on sleep (Chen et al., 2019). This supports a framework in which many of the identified sleep-regulating neurons may actually be conditionally-recruited loci that allow specific internal and external states to influence immediate sleep/wake probability but do not have major effects on sleep in normal conditions.

We speculate that he γ5β′2a/β′2mp/β′2mp_bilateral MBONs are activated by physiological or environmental factors that reduce sleep in response to competing motivational drives, with *ban* expression acting as the switch to turn neural activity off and on. These MBON neurons are known to be required for behaviors

that might compete with sleep, including avoidance of aversive stimuli, aversion to pathogen-infected food, ingestion, startle-induced locomotion, and memory for visual and olfactory cues (Al-Anzi and Zinn, 2018; Aso et al., 2014b; Kobler et al., 2020; Lewis et al., 2015; Owald et al., 2015; Sun et al., 2018; Yamazaki et al., 2018).

The sleep-promoting effect of *ban* in the γ5β′2a/β′2mp/β′2mp_bilateral MBONs appears to be the result of regulation of several mRNA targets, likely including *CCHamide-2 receptor* and *kelch*. *Kelch* is a BTB-domain adaptor protein for the Cullin-3 ubiquitin E3 ligase that is involved in actin regulation (Hudson and Cooley, 2010; Kelso et al., 2002) and dendritic branching (Djagaeva and Doronkin, 2009). Cullin-3 and *Insomniac*, another BTB-domain adaptor protein, have been previously implicated in sleep (Pfeiffenberger and Allada, 2012). *CCha2-R* is a GPCR for the gut-derived peptide hormone CCHamide-2 which has a critical role in feeding and growth (Ren et al., 2015; Sano et al., 2015). Activation of the CCHa2-R receptor enhances calcium responses in these neuroendocrine cells (Sano et al., 2015), consistent with a role for CCHa2-R in promoting neural activity of MBONs.

Limitations of the study

This study identifies a very small group of adult neurons as regulators of early night sleep. Our use of a validated microRNA sponge strongly suggests expression of *ban* in γ5β′2a/β′2mp/β′2mp_bilateral MBONs but does not directly demonstrate it. In addition, these neurons likely act as context-dependent modulators of sleep rather than required elements for the behavior, so the phenotypes we demonstrate are by their nature small. Because microRNAs typically act on suites of genes, the identification of single *ban* targets as major mediators of its effects on sleep may be difficult if groups of genes are acting synergistically. Future work, examining synergy between targets and carrying out epistasis experiments will likely yield a better understanding of how modulation of the *ban* gene network regulates sleep in these MBONs.

STAR★METHODS

Detailed methods are provided in the online version of this paper and include the following:

- KEY RESOURCES TABLE
- RESOURCE AVAILABILITY
  - Lead contact
  - Materials availability
  - Data and code availability
- EXPERIMENTAL MODEL AND SUBJECT DETAILS
- METHOD DETAILS
  - *Drosophila* lines
  - *Drosophila* husbandry and sleep assay
  - Immunohistochemistry
  - FACS sorting and RNA-seq of MBONs
  - GCaMP6f imaging and antennal lobe stimulation
- QUANTIFICATION AND STATISTICAL ANALYSIS

SUPPLEMENTAL INFORMATION

Supplemental information can be found online at https://doi.org/10.1016/j.isci.2022.104874.

ACKNOWLEDGMENTS

This work was supported by P01NS090994 and R01MH067284 to LCG. MH and EJRR were supported by T32MH019929. Stocks obtained from the Bloomington Drosophila Stock Center (NIH P40 OD018537) were used in this study. We thank Michael Rosbash for support and critical comments on this work.

AUTHOR CONTRIBUTIONS

M.H. and L.C.G. designed the study. M.H., K.D., M.A., E.J.R.R., E.A.K., and D.M. performed experiments and analyzed data. M.H. wrote the original draft and M.H. and L.C.G. edited with input from all authors.

DECLARATION OF INTERESTS

The authors declare no competing interests.

Received: October 13, 2021
Revised: July 7, 2022
Accepted: July 29, 2022
Published: September 16, 2022

REFERENCES

Agarwal, V., Subtelny, A.O., Thiru, P., Ulitsky, I., and Bartel, D.P. (2018). Predicting microRNA targeting efficacy in Drosophila. Genome Biol. *19*, 152. https://doi.org/10.1186/s13059-018-1504-3.

Agosto, J., Choi, J.C., Parisky, K.M., Stilwell, G., Rosbash, M., and Griffith, L.C. (2008). Modulation of $GABA_A$ receptor desensitization uncouples sleep onset and maintenance in *Drosophila*. Nat. Neurosci. *11*, 354–359.

Al-Anzi, B., and Zinn, K. (2018). Identification and characterization of mushroom body neurons that regulate fat storage in Drosophila. Neural Dev. *13*, 18. https://doi.org/10.1186/s13064-018-0116-7.

Aso, Y., Grübel, K., Busch, S., Friedrich, A.B., Siwanowicz, I., and Tanimoto, H. (2009). The mushroom body of adult Drosophila characterized by GAL4 drivers. J. Neurogenet. *23*, 156–172. https://doi.org/10.1080/01677060802471718.

Aso, Y., Hattori, D., Yu, Y., Johnston, R.M., Iyer, N.A., Ngo, T.T.B., Dionne, H., Abbott, L.F., Axel, R., Tanimoto, H., and Rubin, G.M. (2014a). The neuronal architecture of the mushroom body provides a logic for associative learning. Elife *3*, e04577. https://doi.org/10.7554/eLife.04577.

Aso, Y., Sitaraman, D., Ichinose, T., Kaun, K.R., Vogt, K., Belliart-Guérin, G., Plaçais, P.Y., Robie, A.A., Yamagata, N., Schnaitmann, C., et al. (2014b). Mushroom body output neurons encode valence and guide memory-based action selection in Drosophila. Elife *3*, e04580. https://doi.org/10.7554/eLife.04580.

Banerjee, A., and Roy, J.K. (2017). Dicer-1 regulates proliferative potential of Drosophila larval neural stem cells through bantam miRNA based down-regulation of the G1/S inhibitor Dacapo. Dev. Biol. *423*, 57–65. https://doi.org/10.1016/j.ydbio.2017.01.011.

Barnstedt, O., Owald, D., Felsenberg, J., Brain, R., Moszynski, J.P., Talbot, C.B., Perrat, P.N., and Waddell, S. (2016). Memory-relevant mushroom body output synapses are cholinergic. Neuron *89*, 1237–1247. https://doi.org/10.1016/j.neuron.2016.02.015.

Becam, I., Rafel, N., Hong, X., Cohen, S.M., and Milán, M. (2011). Notch-mediated repression of bantam miRNA contributes to boundary formation in the Drosophila wing. Development *138*, 3781–3789. https://doi.org/10.1242/dev.064774.

Bischof, J., Maeda, R.K., Hediger, M., Karch, F., and Basler, K. (2007). An optimized transgenesis system for Drosophila using germ-line-specific phiC31 integrases. Proc. Natl. Acad. Sci. USA *104*, 3312–3317. https://doi.org/10.1073/pnas.0611511104.

Brennecke, J., Hipfner, D.R., Stark, A., Russell, R.B., and Cohen, S.M. (2003). Bantam encodes a developmentally regulated microRNA that controls cell proliferation and regulates the proapoptotic gene hid in Drosophila. Cell *113*, 25–36. https://doi.org/10.1016/s0092-8674(03)00231-9.

Chakravarti Dilley, L., Szuperak, M., Gong, N.N., Williams, C.E., Saldana, R.L., Garbe, D.S., Syed, M.H., Jain, R., and Kayser, M.S. (2020). Identification of a molecular basis for the juvenile sleep state. Elife *9*, e52676. https://doi.org/10.7554/eLife.52676.

Chen, K.F., Lowe, S., Lamaze, A., Krätschmer, P., and Jepson, J. (2019). Neurocalcin regulates nighttime sleep and arousal in Drosophila. Elife *8*, e38114. https://doi.org/10.7554/eLife.38114.

Chen, T.W., Wardill, T.J., Sun, Y., Pulver, S.R., Renninger, S.L., Baohan, A., Schreiter, E.R., Kerr, R.A., Orger, M.B., Jayaraman, V., et al. (2013). Ultrasensitive fluorescent proteins for imaging neuronal activity. Nature *499*, 295–300. https://doi.org/10.1038/nature12354.

Cong, X., Wang, H., Liu, Z., He, C., An, C., and Zhao, Z. (2015). Regulation of sleep by insulin-like peptide system in Drosophila melanogaster. Sleep *38*, 1075–1083. https://doi.org/10.5665/sleep.4816.

Crocker, A., and Sehgal, A. (2010). Genetic analysis of sleep. Genes Dev. *24*, 1220–1235. https://doi.org/10.1101/gad.1913110.

Djagaeva, I., and Doronkin, S. (2009). COP9 limits dendritic branching via Cullin3-dependent degradation of the actin-crosslinking BTB-domain protein Kelch. PLoS One *4*, e7598. https://doi.org/10.1371/journal.pone.0007598.

Dobin, A., Davis, C.A., Schlesinger, F., Drenkow, J., Zaleski, C., Jha, S., Batut, P., Chaisson, M., and Gingeras, T.R. (2013). STAR: ultrafast universal RNA-seq aligner. Bioinformatics *29*, 15–21. https://doi.org/10.1093/bioinformatics/bts635.

Donelson, N.C., Kim, E.Z., Slawson, J.B., Vecsey, C.G., Huber, R., and Griffith, L.C. (2012). High-resolution positional tracking for long-term analysis of Drosophila sleep and locomotion using the "tracker" program. PLoS One *7*, e37250. https://doi.org/10.1371/journal.pone.0037250.

Feng, Y., Ueda, A., and Wu, C.F. (2004). A modified minimal hemolymph-like solution, HL3.1, for physiological recordings at the neuromuscular junctions of normal and mutant Drosophila larvae. J. Neurogenet. *18*, 377–402. https://doi.org/10.1080/01677060490894522.

Friggi-Grelin, F., Coulom, H., Meller, M., Gomez, D., Hirsh, J., and Birman, S. (2003). Targeted gene expression in Drosophila dopaminergic cells using regulatory sequences from tyrosine hydroxylase. J. Neurobiol. *54*, 618–627.

Fulga, T.A., McNeill, E.M., Binari, R., Yelick, J., Blanche, A., Booker, M., Steinkraus, B.R., Schnall-Levin, M., Zhao, Y., DeLuca, T., et al. (2015). A transgenic resource for conditional competitive inhibition of conserved Drosophila microRNAs. Nat. Commun. *6*, 7279. https://doi.org/10.1038/ncomms8279.

Gmeiner, F., Kołodziejczyk, A., Yoshii, T., Rieger, D., Nässel, D.R., and Helfrich-Förster, C. (2013). GABA(B) receptors play an essential role in maintaining sleep during the second half of the night in Drosophila melanogaster. J. Exp. Biol. *216*, 3837–3843. https://doi.org/10.1242/jeb.085563.

Gong, Z.F., Xia, S.Z., Liu, L., Feng, C.H., and Guo, A.K. (1998). Operant visual learning and memory in Drosophila mutants dunce, amnesiac and radish. J. Insect Physiol. *44*, 1149–1158.

Goodwin, P.R., Meng, A., Moore, J., Hobin, M., Fulga, T.A., Van Vactor, D., and Griffith, L.C. (2018). MicroRNAs regulate sleep and sleep homeostasis in Drosophila. Cell Rep. *23*, 3776–3786. https://doi.org/10.1016/j.celrep.2018.05.078.

Hamada, F.N., Rosenzweig, M., Kang, K., Pulver, S.R., Ghezzi, A., Jegla, T.J., and Garrity, P.A. (2008). An internal thermal sensor controlling temperature preference in Drosophila. Nature *454*, 217–220.

Hendricks, J.C., Finn, S.M., Panckeri, K.A., Chavkin, J., Williams, J.A., Sehgal, A., and Pack, A.I. (2000). Rest in Drosophila is a sleep-like state. Neuron *25*, 129–138.

Huang, X., Shi, L., Cao, J., He, F., Li, R., Zhang, Y., Miao, S., Jin, L., Qu, J., Li, Z., and Lin, X. (2014). The sterile 20-like kinase tao controls tissue homeostasis by regulating the hippo pathway in Drosophila adult midgut. J. Genet. Genomics *41*, 429–438. https://doi.org/10.1016/j.jgg.2014.05.007.

Hudson, A.M., and Cooley, L. (2010). Drosophila Kelch functions with Cullin-3 to organize the ring canal actin cytoskeleton. J. Cell Biol. *188*, 29–37. https://doi.org/10.1083/jcb.200909017.

Hudson, A.M., Mannix, K.M., and Cooley, L. (2015). Actin cytoskeletal organization in Drosophila germline ring canals depends on kelch function in a cullin-RING E3 ligase. Genetics *201*, 1117–1131. https://doi.org/10.1534/genetics.115.181289.

Jenett, A., Rubin, G.M., Ngo, T.T.B., Shepherd, D., Murphy, C., Dionne, H., Pfeiffer, B.D., Cavallaro, A., Hall, D., Jeter, J., et al. (2012). A GAL4-driver line resource for Drosophila neurobiology. Cell Rep. *2*, 991–1001. https://doi.org/10.1016/j.celrep.2012.09.011.

Joiner, W.J., Crocker, A., White, B.H., and Sehgal, A. (2006). Sleep in Drosophila is regulated by adult mushroom bodies. Nature *441*, 757–760. https://doi.org/10.1038/nature04811.

Jonas, S., and Izaurralde, E. (2015). Towards a molecular understanding of microRNA-mediated gene silencing. Nat. Rev. Genet. *16*, 421–433. https://doi.org/10.1038/nrg3965.

Kelso, R.J., Hudson, A.M., and Cooley, L. (2002). Drosophila Kelch regulates actin organization via Src64-dependent tyrosine phosphorylation. J. Cell Biol. *156*, 703–713. https://doi.org/10.1083/jcb.200110063.

Kitamoto, T. (2001). Conditional modification of behavior in Drosophila by targeted expression of a temperature-sensitive shibire allele in defined neurons. J. Neurobiol. *47*, 81–92.

Kobler, J.M., Rodriguez Jimenez, F.J., Petcu, I., and Grunwald Kadow, I.C. (2020). Immune receptor signaling and the mushroom body mediate post-ingestion pathogen avoidance. Curr. Biol. *30*, 4693–4709e3. https://doi.org/10.1016/j.cub.2020.09.022.

Kunst, M., Hughes, M.E., Raccuglia, D., Felix, M., Li, M., Barnett, G., Duah, J., and Nitabach, M.N. (2014). Calcitonin gene-related peptide neurons mediate sleep-specific circadian output in Drosophila. Curr. Biol. *24*, 2652–2664. https://doi.org/10.1016/j.cub.2014.09.077.

Lee, T., and Luo, L. (1999). Mosaic analysis with a repressible cell marker for studies of gene function in neuronal morphogenesis. Neuron *22*, 451–461. https://doi.org/10.1016/s0896-6273(00)80701-1.

Lerner, I., Bartok, O., Wolfson, V., Menet, J.S., Weissbein, U., Afik, S., Haimovich, D., Gafni, C., Friedman, N., Rosbash, M., and Kadener, S. (2015). Clk post-transcriptional control denoises circadian transcription both temporally and spatially. Nat. Commun. *6*, 7056. https://doi.org/10.1038/ncomms8056.

Lewis, L.P.C., Siju, K.P., Aso, Y., Friedrich, A.B., Bulteel, A.J.B., Rubin, G.M., and Grunwald Kadow, I.C. (2015). A higher brain circuit for immediate integration of conflicting sensory information in Drosophila. Curr. Biol. *25*, 2203–2214. https://doi.org/10.1016/j.cub.2015.07.015.

Li, H., Horns, F., Wu, B., Xie, Q., Li, J., Li, T., Luginbuhl, D.J., Quake, S.R., and Luo, L. (2017). Classifying Drosophila olfactory projection neuron subtypes by single-cell RNA sequencing. Cell *171*, 1206–1220.e22. https://doi.org/10.1016/j.cell.2017.10.019.

Liu, H., Li, Y., He, J., Guan, Q., Chen, R., Yan, H., Zheng, W., Song, K., Cai, H., Guo, Y., et al. (2017). Robust transcriptional signatures for low-input RNA samples based on relative expression orderings. BMC Genom. *18*, 913. https://doi.org/10.1186/s12864-017-4280-7.

Ma, D., Przybylski, D., Abruzzi, K.C., Schlichting, M., Li, Q., Long, X., and Rosbash, M. (2021). A transcriptomic taxonomy of Drosophila circadian neurons around the clock. Elife *10*, e63056. https://doi.org/10.7554/eLife.63056.

Mao, Z., and Davis, R.L. (2009). Eight different types of dopaminergic neurons innervate the Drosophila mushroom body neuropil: anatomical and physiological heterogeneity. Front. Neural Circuits *3*, 5. https://doi.org/10.3389/neuro.04.005.2009.

McGuire, S.E., Le, P.T., Osborn, A.J., Matsumoto, K., and Davis, R.L. (2003). Spatiotemporal rescue of memory dysfunction in Drosophila. Science *302*, 1765–1768.

Owald, D., Felsenberg, J., Talbot, C.B., Das, G., Perisse, E., Huetteroth, W., and Waddell, S. (2015). Activity of defined mushroom body output neurons underlies learned olfactory behavior in Drosophila. Neuron *86*, 417–427. https://doi.org/10.1016/j.neuron.2015.03.025.

Paraskevopoulou, M.D., Georgakilas, G., Kostoulas, N., Vlachos, I.S., Vergoulis, T., Reczko, M., Filippidis, C., Dalamagas, T., and Hatzigeorgiou, A.G. (2013). DIANA-microT web server v5.0: service integration into miRNA functional analysis workflows. Nucleic Acids Res. *41*, W169–W173. https://doi.org/10.1093/nar/gkt393.

Parrish, J.Z., Xu, P., Kim, C.C., Jan, L.Y., and Jan, Y.N. (2009). The microRNA bantam functions in epithelial cells to regulate scaling growth of dendrite arbors in drosophila sensory neurons. Neuron *63*, 788–802. https://doi.org/10.1016/j.neuron.2009.08.006.

Pfeiffenberger, C., and Allada, R. (2012). Cul3 and the BTB adaptor insomniac are key regulators of sleep homeostasis and a dopamine arousal pathway in Drosophila. PLoS Genet. *8*, e1003003. https://doi.org/10.1371/journal.pgen.1003003.

Pfeiffer, B.D., Truman, J.W., and Rubin, G.M. (2012). Using translational enhancers to increase transgene expression in Drosophila. Proc. Natl. Acad. Sci. USA *109*, 6626–6631. https://doi.org/10.1073/pnas.1204520109.

Picelli, S., Faridani, O.R., Björklund, A.K., Winberg, G., Sagasser, S., and Sandberg, R. (2014). Full-length RNA-seq from single cells using Smart-seq2. Nat. Protoc. *9*, 171–181. https://doi.org/10.1038/nprot.2014.006.

Pitman, J.L., McGill, J.J., Keegan, K.P., and Allada, R. (2006). A dynamic role for the mushroom bodies in promoting sleep in Drosophila. Nature *441*, 753–756. https://doi.org/10.1038/nature04739.

Plihal, W., and Born, J. (1997). Effects of early and late nocturnal sleep on declarative and procedural memory. J. Cogn. Neurosci. *9*, 534–547. https://doi.org/10.1162/jocn.1997.9.4.534.

Reczko, M., Maragkakis, M., Alexiou, P., Grosse, I., and Hatzigeorgiou, A.G. (2012). Functional microRNA targets in protein coding sequences. Bioinformatics *28*, 771–776. https://doi.org/10.1093/bioinformatics/bts043.

Ren, G.R., Hauser, F., Rewitz, K.F., Kondo, S., Engelbrecht, A.F., Didriksen, A.K., Schjøtt, S.R., Sembach, F.E., Li, S., Søgaard, K.C., et al. (2015). CCHamide-2 is an orexigenic brain-gut peptide in Drosophila. PLoS One *10*, e0133017. https://doi.org/10.1371/journal.pone.0133017.

Robinson, M.D., McCarthy, D.J., and Smyth, G.K. (2010). edgeR: a Bioconductor package for differential expression analysis of digital gene expression data. Bioinformatics *26*, 139–140. https://doi.org/10.1093/bioinformatics/btp616.

Ruby, J.G., Stark, A., Johnston, W.K., Kellis, M., Bartel, D.P., and Lai, E.C. (2007). Evolution, biogenesis, expression, and target predictions of a substantially expanded set of Drosophila microRNAs. Genome Res. *17*, 1850–1864. https://doi.org/10.1101/gr.6597907.

Sano, H., Nakamura, A., Texada, M.J., Truman, J.W., Ishimoto, H., Kamikouchi, A., Nibu, Y., Kume, K., Ida, T., and Kojima, M. (2015). The nutrient-responsive hormone CCHamide-2 controls growth by regulating insulin-like peptides in the brain of Drosophila melanogaster. PLoS Genet. *11*, e1005209. https://doi.org/10.1371/journal.pgen.1005209.

Shafer, O.T., and Keene, A.C. (2021). The regulation of Drosophila sleep. Curr. Biol. *31*, R38–R49. https://doi.org/10.1016/j.cub.2020.10.082.

Shaw, P.J., Cirelli, C., Greenspan, R.J., and Tononi, G. (2000). Correlates of sleep and waking in *Drosophila melanogaster*. Science *287*, 1834–1837.

Shcherbata, H.R., Ward, E.J., Fischer, K.A., Yu, J.Y., Reynolds, S.H., Chen, C.H., Xu, P., Hay, B.A., and Ruohola-Baker, H. (2007). Stage-specific differences in the requirements for germline stem cell maintenance in the Drosophila ovary. Cell Stem Cell *1*, 698–709. https://doi.org/10.1016/j.stem.2007.11.007.

Sitaraman, D., Aso, Y., Jin, X., Chen, N., Felix, M., Rubin, G.M., and Nitabach, M.N. (2015). Propagation of homeostatic sleep signals by segregated synaptic microcircuits of the Drosophila mushroom body. Curr. Biol. *25*, 2915–2927. https://doi.org/10.1016/j.cub.2015.09.017.

Song, Y., Ori-McKenney, K.M., Zheng, Y., Han, C., Jan, L.Y., and Jan, Y.N. (2012). Regeneration of Drosophila sensory neuron axons and dendrites is regulated by the Akt pathway involving Pten and microRNA bantam. Genes Dev. *26*, 1612–1625. https://doi.org/10.1101/gad.193243.112.

Sun, J., Xu, A.Q., Giraud, J., Poppinga, H., Riemensperger, T., Fiala, A., and Birman, S. (2018). Neural control of startle-induced locomotion by the mushroom bodies and associated neurons in Drosophila. Front. Syst. Neurosci. *12*, 6. https://doi.org/10.3389/fnsys.2018.00006.

Ueno, K., Naganos, S., Hirano, Y., Horiuchi, J., and Saitoe, M. (2013). Long-term enhancement of synaptic transmission between antennal lobe and mushroom body in cultured Drosophila brain. J. Physiol. *591*, 287–302. https://doi.org/10.1113/jphysiol.2012.242909.

Ueno, K., Suzuki, E., Naganos, S., Ofusa, K., Horiuchi, J., and Saitoe, M. (2017). Coincident postsynaptic activity gates presynaptic dopamine release to induce plasticity in Drosophila mushroom bodies. Elife *6*, e21076. https://doi.org/10.7554/eLife.21076.

Wang, Y., Mamiya, A., Chiang, A.S., and Zhong, Y. (2008). Imaging of an early memory trace in the Drosophila mushroom body. J. Neurosci. *28*,

4368–4376. https://doi.org/10.1523/JNEUROSCI.2958-07.2008.

Weng, R., and Cohen, S.M. (2015). Control of Drosophila Type I and Type II central brain neuroblast proliferation by bantam microRNA. Development *142*, 3713–3720. https://doi.org/10.1242/dev.127209.

Wiggin, T.D., Goodwin, P.R., Donelson, N.C., Liu, C., Trinh, K., Sanyal, S., and Griffith, L.C. (2020). Covert sleep-related biological processes are revealed by probabilistic analysis in Drosophila. Proc. Natl. Acad. Sci. USA *117*, 10024–10034. https://doi.org/10.1073/pnas.1917573117.

Xie, X., Tabuchi, M., Corver, A., Duan, G., Wu, M.N., and Kolodkin, A.L. (2019). Semaphorin 2b regulates sleep-circuit formation in the Drosophila central brain. Neuron *104*, 322–337e14. https://doi.org/10.1016/j.neuron.2019.07.019.

Yamazaki, D., Hiroi, M., Abe, T., Shimizu, K., Minami-Ohtsubo, M., Maeyama, Y., Horiuchi, J., and Tabata, T. (2018). Two parallel pathways assign opposing odor valences during Drosophila memory formation. Cell Rep. *22*, 2346–2358. https://doi.org/10.1016/j.celrep.2018.02.012.

Yordanova, J., Kolev, V., Verleger, R., Bataghva, Z., Born, J., and Wagner, U. (2008). Shifting from implicit to explicit knowledge: different roles of early- and late-night sleep. Learn. Mem. *15*, 508–515. https://doi.org/10.1101/lm.897908.

STAR★METHODS

KEY RESOURCES TABLE

REAGENT or RESOURCE	SOURCE	IDENTIFIER
Antibodies		
Anti-GFP	Invitrogen	Cat# A-11122 RRID: AB_221569
anti-BRP	DSHB	nc82; RRID: AB_2314866
Alexa Fluor 488 (goat anti-rabbit)	Invitrogen	Cat# A-11008 RRID: AB_143165
Alexa Fluor 633 (goat anti-mouse)	Invitrogen	Cat# A-21052 RRID:AB_2535719
Vectashield	Vector Laboratories, Inc.	Cat# H-1000 RRID: AB_2336789
Chemicals, peptides, and recombinant proteins		
Tetrodotoxin (TTX)	Tocris Bioscience	Cat# 1078
Papain	Worthington	Cat# LK003176
Agencourt AMPure XP beads	Beckman Coulter	Cat# A63880
Critical commercial assays		
Dynabead mRNA Direct Purification kit	Invitrogen	Cat# 61,011
Nextera XT DNA Library Preparation Kit	Illumina	Cat# FC-131-1096
Experimental models: Organisms/strains		
UAS-ban-SP	Becam et al., 2011	N/A
UAS-scamble-SP	BDSC	#61501
UAS-CD8::GFP	Lee and Luo, 1999	N/A
20XUAS-GCaMP6f	BDSC	#52869
pJFRC124-20XUAS-IVS-dTrpA1	Gift from Janelia	N/A
UAS-kelch	Hudson et al., 2015	N/A
20XUAS-GCaMP6f	BDSC	#52869
20xUAS-IVS-Syn21-Shi^{ts}	Pfeiffer et al., 2012	N/A
UAS-Ugt36D1	This paper	N/A
UAS-CCHa2-R	This paper	N/A
nsyb-GAL4	BDSC	#51941
bantam-GAL4	Gift from Sebastian Kadener	N/A
OK107-GAL4	BDSC	#854
TH-GAL4	BDSC	#8848
GMR14C08-GAL4	BDSC	#48606
MB011B Split-GAL4	BDSC	#68294
tubulin-GAL80^{ts}	BDSC	#7019
RNA seq data set	GEO	GSE208649
Oligonucleotides		
CCHa2-R mRNA forward primer for cloning	AGTCCTGTGCACGGATTC	N/A
CCHa2-R mRNA reverse primer for cloning	ACATTTATGGAATCCATTTATTTACATTAA	N/A
Ugt36D1 mRNA forward primer for cloning	TTTCATTCGGATGTAGTCTCC	N/A
Ugt36D1 mRNA reverse primer for cloning	ATTTTAAAAACTTTATTTATTTCCGTACTAG	N/A
Recombinant DNA		
pUASTattB	Addgene	GenBank: EF362409.1

(*Continued on next page*)

Continued

REAGENT or RESOURCE	SOURCE	IDENTIFIER
Software and algorithms		
Fiji	http://fiji.sc	RRID: SCR_002285
GraphPad Prism	GraphPad Software	RRID: SCR_002798
MATLAB R2012b	MathWorks	RRID: SCR_001622
Leica TCS SP5	SP5 confocal microscope	RRID: SCR_002140

RESOURCE AVAILABILITY

Lead contact

Further information and requests for resources and reagents should be directed to and will be fulfilled by the lead contact, Leslie C. Griffith (griffith@brandeis.edu).

Materials availability

Newly generated transgenic lines available on request to lead contact.

Data and code availability

- The datasets supporting this manuscript are available on request directed to the lead contact.
- This paper does not report original code.
- The RNA seq data have been deposited at GEO (accession number GEO: GSE208649). Any additional information required to reanalyze the data reported in this paper is available from the lead contact on request.

EXPERIMENTAL MODEL AND SUBJECT DETAILS

Adult mated female *Drosophila melanogaster* (~4–10 days old) were employed in all studies except where noted.

METHOD DETAILS

Drosophila lines

UAS lines include *UAS-ban-SP* and *UAS-scramble-SP* (Fulga et al., 2015), *UAS-CD8::GFP* (Lee and Luo, 1999), *UAS-kelch* (Hudson et al., 2015), *20XUAS-GCaMP6f* (Chen et al., 2013), *20XUAS-IVS-dTrpA1* and *20xUAS-IVS-Syn21-Shi^{ts}* (Pfeiffer et al., 2012). *UAS-Ugt36D1* and *UAS-CCha2-R* lines were generated by cloning their cDNA-derived mRNA sequences into the *Drosophila* expression vector *pUASTattB* which was then integrated into the attp40 PhiC31 integration site on chromosome 2 (Bischof et al., 2007). Injections were performed by Rainbow Transgenic Flies Inc (Camarillo, CA).GAL4s include *nSyb-GAL4*, *ban-Gal4* (generous gift of Sebastian Kadener, Brandeis University), *OK107-GAL4* (Aso et al., 2009), *TH-GAL4* (Friggi-Grelin et al., 2003) and *GMR14C08-GAL4* (Jenett et al., 2012). Split-GAL4s include *MB011B* (Aso et al., 2014a). GAL80 lines include *tubulin-GAL80^{ts}* (McGuire et al., 2003).

Drosophila husbandry and sleep assay

Flies were grown on standard cornmeal/agar food supplemented with yeast. *Drosophila* Activity Monitor (DAM) system (TriKinetics, Waltham) was used to measure sleep (Donelson et al., 2012). Female flies were loaded into glass sleep tubes containing a food mixture of 5% sucrose and 2% agar. Young female flies were housed with w^{1118} males >24 h before loading in sleep tubes in order to ensure that flies were mated. Temperature was kept constant at 25°C throughout sleep recording unless otherwise noted. Flies were considered sleeping if they were inactive for 5 min or more (Hendricks et al., 2000; Shaw et al., 2000). Sleep was averaged across 2–5 days unless otherwise noted. DAM data was analyzed using a custom MATLAB program called Sleep and Circadian Analysis MATLAB Program (SCAMP) (Donelson et al., 2012). The NAMEAN measure (beam breaks per active minute) was used to assess basal locomotor behavior. For all sleep duration data, a D'Agostino-Pearson test was used to test for normality. If normally distributed, data was analyzed with ANOVA or T-test depending on the number of groups. If not normally distributed,

data was analyzed with a Kruskal-Wallis ANOVA with Dunn's multiple comparison test or with a Mann-Whitney test. Statistics were performed using GraphPad Prism.

Immunohistochemistry

Fly brains were dissected in ice cold Schneider's Insect Medium (S2) and fixed in 2% paraformaldehyde for 55 min at room temperature. Brains were then washed 4X in PBS with .5% Triton X-100 (PBS-T) and then placed in blocking solution (PBS-T with 5% normal goat serum (NGS; Invitrogen)) for 90 min at room temperature. Incubation in primary and secondary antibodies was performed for 2–3 days at 4°C. Anti-GFP (raised in rabbit; Invitrogen) and anti-BRP (raised in mouse; monoclonal Nc82) were used at concentrations 1:1000 and 1:25, respectively. Anti-rabbit Alexa Flour 488 and anti-mouse Alexa Flour 633 (both Invitrogen) were used at 1:500. Brains were then washed 4X times in PBS-T and placed in 2% paraformaldehyde for 4 h at room temperature. Brains were washed 4X times in PBS-T and then mounted using Vectashield Mounting Medium (Vector Laboratories). Slides were imaged on a Leica SP5 confocal microscope with a 63x objective. Maximum intensity Z projections were generated using FIJI software.

FACS sorting and RNA-seq of MBONs

FACS was performed using a previously described protocol (Ma et al., 2021). The brains of *MB011B>UAS-CD8::GFP+UAS-ban-SP* and control *MB011B>UAS-CD8::GFP+UAS-scr-SP* mated female flies (3–4 days after eclosion) were dissected between ZT12 and ZT13:30 in artificial hemolymph (AHL- 108 mM NaCl, 5 mM KCl, 2 mM CaCl2, 8.2 mM MgCl2, 4 mM NaHCO3, 1 mM NaH2PO4-H2O, 5 mM trehalose, 10 mM sucrose, 5 mM HEPES; pH 7.5) and 0.1 μM tetrodotoxin (TTX). Brains were collected in SM medium (active Schneider's medium) and 0.1 μM TTX. Brains were then digested in Papain (Worthington PAP2, 50 unit/mL, with approximately 2 μL per brain) for 30 min and then quenched with 5X volume of SM media+TTX. Trituration was performed with flame-rounded 1000 μl and 200 μL pipette tips. Filtration was performed with a 100 μm sieve. Cell sorting was performed using a BD FACS Melody using the GFP channel. Sorted cells were collected in an Eppendorf tube with 50μL lysis buffer (Dynabead mRNA Direct Purification kit, Invitrogen) and stored at −80°C.

RNA sequencing was performed using a modified SMART-seq2 protocol (Li et al., 2017; Picelli et al., 2014). Briefly, mRNA was isolated from cells using a Dynabead mRNA purification kit (Invitrogen). Poly(A)-tailed RNA was reverse transcribed and PCR-amplified with 25 cycles. cDNA libraries were cleaned using AMPure beads (Agencourt). The resulting full-length cDNA was used as the input to the tagmentation based Nextera XT (Illumina) protocol to generate sequencing libraries. Two biological replications were sequenced on a Next-seq 500 platform with paired-end 75bp reads and one biological replication was sequenced on a Hi-seq platform with paired-end 150bp reads. Reads were aligned to the *Drosophila* genome (dm6) using STAR (Dobin et al., 2013). EdgeR was used to perform DGE on the aligned reads of the three biological replicates (Robinson et al., 2010). The list of predicted *ban* targets was generated by TargetscanFly7.2 (Agarwal et al., 2018; Ruby et al., 2007) and DIANA-microT (Paraskevopoulou et al., 2013; Reczko et al., 2012) using an miTG threshold of .5.

GCaMP6f imaging and antennal lobe stimulation

Calcium imaging was performed using a modified version of a previously published protocol (Ueno et al., 2013). All imaged flies were mated females, 4–5 days after eclosion. *GMR14C08>UAS-ban-SP+GCaMP6f* and *GMR14C08>UAS-scr-SP+GCaMP6f* brains were dissected in ice cold HL3.1 (Feng et al., 2004) and loaded into a recording chamber submerged in HL3.1. A glass microelectrode was used to stimulate one antennal lobe. The microelectrode was approximately one fourth the size of the antennal lobe. The microelectrode delivered a stimulation train of 20 0.12mA pulses at 100 Hz with a pulse width of 1 millisecond (ms) and an inter-pulse interval of 9 ms.

Simultaneously, GCaMP signals were recorded from the dendritic arborizations of the β′2a/β′2mp/β′2mp_bilateral MBONs (identifiable by their distinct morphology). Imaging data was collected at an acquisition rate of 10 Hz (100 millisecond exposure) at a 512x512 resolution using an Olympus microscope with a 40x objective. Only MBON dendrites ipsilateral to the stimulated Antennal Lobe were included in analysis. A ΔF/F0 was calculated for the baseline period (5 s before stimulus onset) and the max calcium response during antennal lobe stimulation. Statistical analysis (two-way ANOVA with Sidak post hoc test) was performed using GraphPad Prism.

QUANTIFICATION AND STATISTICAL ANALYSIS

Statistical analysis was performed using GraphPad Prism. Information about statistical analysis (statistical tests, quantifications and n-values) for individual experiments may be found in their respective figure legends and method details. n-value refers to the number of flies employed per condition per experiment.